Transparent magnetoelectric composites

R. Polícia[a], A. C. Lima[a,b], N. Pereira[a,c], E. Calle[d], M. Vázquez[d], S. Lanceros-Mendez[a,e,f,] and P. Martins[a,g,*]*

[a]Centro/Departamento de Física, Universidade do Minho, 4710-057 Braga, Portugal
[b]INL- International Iberian Nanotechnology Laboratory, 4715-330 Braga, Portugal
[c]Centro Algoritmi, Universidade do Minho, 4800-058 Guimarães, Portugal
[d]Instituto de Ciencia de Materiales de Madrid, CSIC. 28049 Madrid. Spain
[e]BCMaterials, Basque Center for Materials, Applications and Nanostructures, UPV/EHU Science Park, 48940 Leioa, Spain
[f]IKERBASQUE, Basque Foundation for Science, 48013 Bilbao, Spain
[g]IB-S Institute of Science And Innovation for Sustainability, Universidade do Minho, 4710-057, Braga, Portugal

[*]senentxu.lanceros@bcmaterials.net
[*]pmartins@fisica.uminho.pt

The need of flexible and transparent smart materials is leading to substantial advances in principles, material combinations and technologies. Particularly, the development of optically transparent magnetoelectric (ME) materials will open the range of applications to new directions such as transparent sensors, touch display panels, multifunctional flat panel displays and optical magnetic coatings. In this work, a flexible and transparent ME composite is made of magnetostrictive $Fe_{72.5}Si_{12.5}B_{15}$ microwires and piezoelectric P(VDF-TrFE). The high magnetostriction of $Fe_{72.5}Si_{12.5}B_{15}$ (35 ppm) enables superior ME voltage response (65 $mV.cm^{-1}.Oe^{-1}$) obtained at the critical longitudinal magnetic field equating the transverse anisotropy (14500 $A.m^{-1}$) on the external shell of the microwire.

1. Introduction

Magnetoelectric (ME) materials present large potential in scientific and technological applications due to their ability to change the electric polarization in response to an external magnetic field or to change their magnetization in response to an applied electric field.[1] Single-phase ME materials are sparse in nature and have limited applications, since they show weak ME response at very low operating temperatures.[2-4] Alternatively, multiferroic composite materials, with an extrinsically ME effect, are suitable for

practical applications due to the simplicity of the manufacturing process, and, more importantly, large magnitude of ME response at room temperature.[5] These ME heterostructures enable the conversion between magnetic and electrical energies through mechanical coupling between magnetostrictive and piezoelectric phases, allowing a high number of applications including magnetic sensors, actuators, switches, energy harvesters and data storage devices for smart electronic applications.[6,7]

However, despite the large potential of ME materials and the extensive research in this field in the last few years, the search for a flexible and resistant composite with high ME response, low-cost and simple fabrication continues to be a scientific/technological challenge.[8] Flexible materials allow to expand the boundaries of design and packaging, being suitable for a new generation of electronic device applications[9]. Polymer-based composites are the obvious choice to develop this kind of materials[10]. Although ceramic-based ME composites present ME coefficients three orders of magnitude higher than polymer-based ME materials, piezoelectric ceramics are more expensive, rigid, and fragile, which makes them inadequate for several applications.[11] In contrast, polymer-based composites are flexible, light-weight, able to conform into a variety of forms, cheap, require low temperatures to process, and their fabrication can be scaled up, since the production methods are compatible with industrial requirements.[12,13] Among polymeric piezoelectric materials, poly(vinylidene fluoride/ trifluoroethylene), P(VDF-TrFE), a co-polymer of PVDF has been widely studied and used as organic matrix in ME composites since it exhibits high piezoelectric coefficient, stable mechanical properties, high breakdown strength, easy processing, high thermal stability, optical transparency and biocompatibility.[14] Recent results demonstrate the increased potential of polymer-based ME materials and a strong effort is being made to develop new devices such as energy harvesters, actuators, low-temperature spintronics and magnetic sensors, among others.[10,15,16]

As a disruptive approach in this field, the development of optically transparent ME materials will expand the range of applications, namely transparent magnetic sensors, touch display panels, multifunctional flat panel displays and optical magnetic coatings.[17-21] Different flexible and transparent smart materials have already being studied and developed. Thus, magnetic, conductive, and piezoelectric materials which are also flexible and transparent to the visible light are mentioned in the literature[22-25], however, transparent and flexible ME materials capable of combining magnetic and electrical properties on a single compound are still under-explored. A first approach was presented

in [26] , where transparent magnetoelectric (ME) nanocomposites based on magnetostrictive nanowires (NWs) of Fe, Ni and Galfenol dispersed and magnetically aligned inside of a piezoelectric polymer matrix of P(VDF-TrFE) were produced. Yet, the transparency of the material was not quantified and ….

The main difficult in developing a flexible transparent ME materials is related to the magnetostrictive phase. Magnetic particles with high magnetostrictive values, such as $CoFe_2O_4$, for example, are opaque from a certain concentration (higher than 10 weight percentage (wt.%)) hindering the development of a material with high ME response and significant transparency, simultaneously. Herein, we introduce magnetic microwires (MWs) that can be solution to this scenario due to their excellent magnetic properties and unique geometrical features[27] that allow the development of transparent composites. These microwires, particularly those based on FeSiB alloy composition, exhibit a high saturation magnetic polarization (i.e., Js ≈ 1.65 T) and relatively high magnetostriction value ($\lambda_s \approx 35$ppm). Their cylindrical geometry is characterized by a high aspect ratio (i.e., up to meters long and typically, 5-10 μm diameter), that favours the mechanical coupling with the piezoelectric polymer phase. In addition, these microwires, being structurally amorphous, present a strong uniaxial longitudinal magnetoelastic anisotropy determined by the coupling between the internal mechanical stresses and the magnetostriction constant that adds to their shape anisotropy. The magnetization process consists essentially in the nucleation and fast propagation of a single domain wall at relatively low applied field[28,29]. The combination of the geometrical and mechanical properties together with the soft magnetic behaviour makes them suitable for smart applications[27,30]. Indeed, polymer composites incorporating ferromagnetic microwires reveal a series of potential applications due to the flexibility and sensitive response towards external stimuli, such as magnetic field, temperature, or mechanical stress, among others.[31]

In this paper, we present the first flexible and transparent ME material made up of FeSiB amorphous microwires embedded and magnetically aligned inside a piezoelectric matrix of P(VDF-TrFE).

2. Experimental

2.1 Materials

N,N-dimethylformamide (DMF), pure grade was supplied by Fluka and (PVDF-TrFE) (Solef 1010) was supplied by Solvay. All the chemicals and particles were used as received from the suppliers. Poly(3,4-ethylenedioxythiophene)-poly(styrenesulfonate) (PEDOT) 5.0 wt. % conductive screen printable ink was purchased from Sigma-Aldrich.

2.2 Preparation of magnetic microwires and magnetoelectric composite

Glass-coated amorphous microwires were fabricated by quenching and drawing technique[27] having nominal composition of $Fe_{72.5}Si_{12.5}B_{15}$, with 9.2 μm metallic diameter and coated by Pyrex to a total diameter of 26.2 μm. 20 pieces of microwires (≈4cm) have been placed in parallel and with a 2 mm spacing on a clean glass substrate. 2 g of P(VDF-TrFE) have been added to DMF and mechanical agitation has been performed until a complete dissolution of the polymer. The resulting solution was homogeneously distributed with a spreader over the aligned micowires. After the spreading step, the samples were placed inside an oven (JP Selecta, Model 2000208) for 10 minutes at a temperature of 210 ° C, following the protocol presented in xxx, for polymer melting and complete removal of the solvent. Then, the films (≈ 90 μm) were removed from the oven and allowed to cool at room temperature. The detachment of the flexible composite was obtained after the glass substrate was immersed in a vat for 20 minutes.
XXX

2.3 Characterization

The poling of the samples was achieved, after an optimization procedure[32], after 60 min of corona poling at 120 ˚C in a home-made chamber. In order to optimize the piezoelectric response, the electric field was kept applied when the samples were cooled to room temperature. The piezoelectric response (d_{33}) of the poled samples was obtained with a wide range d33-meter (model 8000, APC Int. Ltd).

The magnetic characterization of the microwires was performed in a vibrating sample magnetometer (VSM) (ADE system EV7 KLA-Tencor) under a maximum applied magnetic field of ±1.44 M $A.m^{-1}$, parallel to the microwire axis.

ME effect was characterized by measuring the transversal ME voltage coefficient (α_{33}) using the dynamic lock-in amplifier method.[32] A pair of Helmholtz coils was used to generate an AC magnetic field with amplitude of 63 $A.m^{-1}$ and frequency of ≈17-28 kHz (resonance of the composites) that is superimposed to a DC bias field driven by an

electromagnet. Both fields are applied out of plane of the nanocomposite film and the generated voltage across the sample thickness is measured using a digital Lock-in amplifier (Stanford Research SR530). The ME voltage coefficient (α_{33}) was calculated from the measured voltage using the equation 1:

$$\alpha_{33} = \frac{\Delta V}{H_{AC} \times t} \qquad (1)$$

where ΔV is the measured output voltage, H_{AC} is the amplitude of the AC magnetic field in Oe, and t is the thickness of the nanocomposite film.

The optical transmittance of the samples was obtained by a double beam spectrophotometer UV-2501PC UltravioleteVisible (UVeVIS) set up in the 350-700 nm range with a 1 nm step.

3. Results and Discussion

Figure 1 depicts the ferromagnetic behaviour of the FeSiB microwires under longitudinal applied field characterized by a squared hysteresis loop with a 182 $A.m^{-1}$ coercivity and a giant Barkhausen jump at around 200 $A.m^{-1}$ applied magnetic field. The square hysteresis loop is characteristic of a bistable magnetic configuration, meaning that at remanence the microwire consists of a large magnetic domain with axial magnetization, and a smaller region (close to the external shell) remaining transversely magnetized. Upon application of a critical field (±200 $A.m^{-1}$), the magnetization reverses in that domain by the fast propagation of a single domain wall. At higher applied field, magnetization increases reversibly at that external shell with small magnetic susceptibility until reaching apparent saturation at above 1.1 M $A.m^{-1}$ applied field.

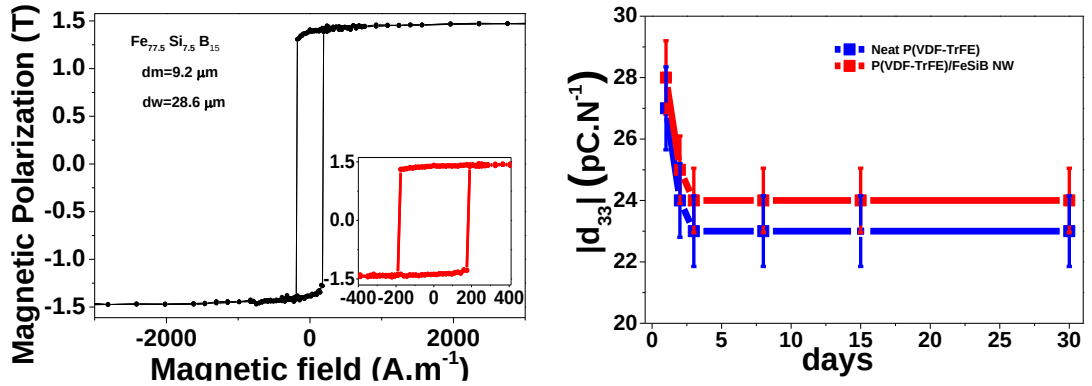

Figure 1. Room-temperature magnetic response of the FeSiB microwires and room-temperature piezoelectric $|d_{33}|$ response of the P(VDF-TrFE)/FeSiB composite.

As the P(VDF-TrFE) matrix has no influence in the type of magnetic response of the magnetostrictive inclusions[10,33], the FeSiB microwires have been introduced in P(VDF-TrFE) and the room-temperature piezoelectric $|d_{33}|$ response of the resulting composite has been studied (Figure 1b). It is observed that the piezoelectric response of the piezoelectric layer is not affected by the introduction of the magnetic fillers once it is similar to the one obtained in the neat P(VDF-TrFE) (24-28 $pC.N^{-1}$).[34]

After the magnetic and piezoelectric behaviour has been verified, the optical transmittance was studied (Figure 2).

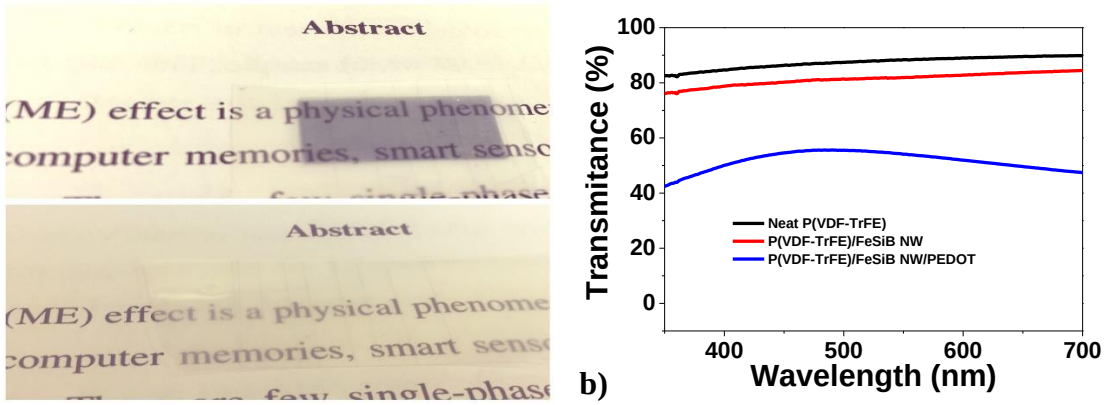

Figure 2. a) Photographs of the composite placed on a written page, with (TOP) and without (DOWN) the PEDOT conductive layers, serving as electrodes. Optical transmittance of the composites measured from 350nm to 700nm.

Figure 2b quantifies the optical transmittance loss from, ≈82% to ≈50%, observed when the two PEDOT conductive layers are printed in the composite. The difference on the optical transmittance between the neat P(VDF-TrFE) (≈88%) and the P(VDF-

TrFE)/FeSiB composite (≈82%) is almost negligible, showing that the optimization of the transmittance in this type of material passes through the optimization of the conductive material and not so much through the optimization of the ME composites composition.

To validate the use of the composite as a ME material for sensor or energy harvesting applications, among others, the room-temperature ME response of the P(VDF-TrFE)/FeSiB/PEDOT was studied as a function of the B_{AC} frequency and DC (B_{DC}) magnetic field.

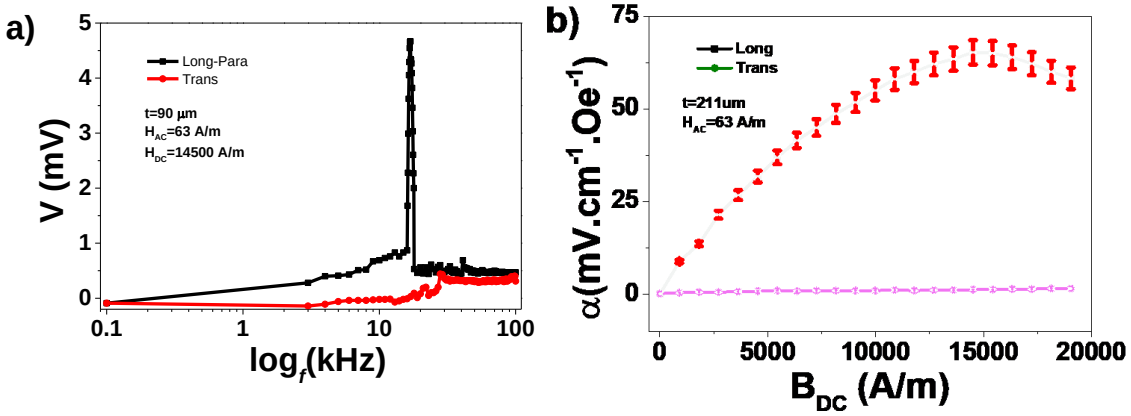

Figure 3. a) ME voltage coefficient (α_{33}) of the sample measured longitudinally (in-plane) and transversally (out-of-plane) as a function of the resonance frequency; b) ME voltage of the sample measured in-plane and out-of-plane as a function of the DC magnetic field.

It is observed that the resonance frequency of the composites is ≈17 kHz when the measurement is performed longitudinally and ≈28kHz when it is performed transversely. It is also observed that the ME voltage response is highly dependent on the direction of the applied magnetic field, reaching a maximum response of 65 $mV.cm^{-1}.Oe^{-1}$ at 14500 $A.m^{-1}$ DC magnetic field and 60 $A.m^{-1}$ AC magnetic field for the sample, when characterized longitudinally. The transversal ME response is negligible. Such distinct response is fully attributed to the small transversal susceptibility of the microwires as a result of the strong uniaxial longitudinal magnetic anisotropy of the microwire. Thus, a quite large transverse applied field is required to observe an even small magnetic response. The bistable magnetic configuration of the microwires (a large magnetic domain with axial magnetization and a transversal magnetization in relatively small region, close to the external shell), ensures that the reversal occurring at 200 $A.m^{-1}$ by the fast propagation of a domain wall does not induce any magnetostrictive effect which is activated only by magnetization rotation mechanisms.

XXXX

Finally, from a simple analysis of the longitudinal applied field at which maximum ME response is obtained we derive an interesting additional conclusion: the applied field can be correlated with the transverse magnetoelastic anisotropy field ($H_{t,max} \approx 14500$ A.m^{-1}) of the microwire that arises from the transverse mechanical stress frozen-in during the quenching fabrication process. Thus, the transverse magnetoelastic anisotropy energy density can be expressed as

$$K_t = (1/2)\, J_s \times H_{t,max} = (3/2)\, \lambda_s \times \langle\sigma\rangle \qquad (2)$$

where $\langle\sigma\rangle$ denotes the average compressive stresses in the external shell. From the experimental data we obtain $\langle\sigma\rangle \approx 230$ MPa which is a quite reasonable value for glass-coated microwires.

In conclusion, the maximum ME response is obtained at the critical longitudinal applied field equating the transverse anisotropy field at the external shell of the microwire. That allows us to anticipate that such a maximum ME can be engineered by the designed choice of the magnetostrictive character of the amorphous microwire (given by the alloy composition) together with the value of the internal mechanical stresses (that can be tailored by suitable thermomagnetic annealing).

4 Conclusion

XXX

ACKNOWLEDGMENT

The authors thank the FCT- Fundação para a Ciência e Tecnologia- for financial support in the framework of the Strategic Funding UID/FIS/04650/2013 and under project PTDC/EEI-SII/5582/2014. P.M., A.C.L. and N.C. acknowledges also support from FCT (SFRH/BPD/96227/2013, SFRH/BD/132624/2017, and SFRH/BD/131729/2017 grants respectively). Financial support from MINECO- MAT2016-76039-C4-3-R

(AEI/FEDER, UE), Basque Government - ELKARTEK and HAZITEK and PIBA (PIBA-2018-06) programs are also acknowledged. Financial support under the project S2018/NMT-4321 NANOMAGCOST-CM from the Regional Government of Madrid is acknowledged.

References

(1) Palneedi, H.; Annapureddy, V.; Priya, S.; Ryu, J. *Actuators* **2016**, *5*.

(2) Folen, V. J.; Rado, G. T.; Stalder, E. W. *Physical Review Letters* **1961**, *6*, 607.

(3) Rado, G. T.; Folen, V. J. *Physical Review Letters* **1961**, *7*, 310.

(4) Schmid, H. *Ferroelectrics* **1994**, *162*, 317.

(5) Nan, C.-W.; Bichurin, M. I.; Dong, S.; Viehland, D.; Srinivasan, G. *Journal of Applied Physics* **2008**, *103*, 031101.

(6) Wang, J.; Neaton, J. B.; Zheng, H.; Nagarajan, V.; Ogale, S. B.; Liu, B.; Viehland, D.; Vaithyanathan, V.; Schlom, D. G.; Waghmare, U. V.; Spaldin, N. A.; Rabe, K. M.; Wuttig, M.; Ramesh, R. *Science* **2003**, *299*, 1719.

(7) Verma, K. C.; Singh, S.; Tripathi, S. K.; Kotnala, R. K. *Journal of Applied Physics* **2014**, *116*, 124103.

(8) Kambale, R. C.; Jeong, D.-Y.; Ryu, J. *Advances in Condensed Matter Physics* **2012**, *2012*, 15.

(9) Oliveira, J.; Correia, V.; Castro, H.; Martins, P.; Lanceros-Mendez, S. *Additive Manufacturing* **2018**, *21*, 269.

(10) Martins, P.; Lanceros-Méndez, S. *Advanced Functional Materials* **2013**, *23*, 3371.

(11) Lin, Y.; Cai, N.; Zhai, J.; Liu, G.; Nan, C.-W. *Physical Review B* **2005**, *72*, 012405.

(12) Maceiras, A.; Martins, P.; Gonçalves, R.; Botelho, G.; Venkata Ramana, E.; Mendiratta, S. K.; San Sebastián, M.; Vilas, J. L.; Lanceros-Mendez, S.; León, L. M. *European Polymer Journal* **2015**, *64*, 224.

(13) Buchanan, G. R. *Composites Part B: Engineering* **2004**, *35*, 413.

(14) Ling, Q.-D.; Liaw, D.-J.; Zhu, C.; Chan, D. S.-H.; Kang, E.-T.; Neoh, K.-G. *Progress in Polymer Science* **2008**, *33*, 917.

(15) Fusil, S. G., V.; Barthélémy, A.; Bibes, M. *Magnetoelectric Devices for Spintronics*, 2014; Vol. 44.

(16) Phuoc, N. O. C. K. *Applied Physics Letters* **2014**, *105*, 022905.

(17) Al-Dahoudi, N.; Bisht, H.; Göbbert, C.; Krajewski, T.; Aegerter, M. *Transparent Conducting, Anti-static and Anti-static–Anti-glare Coatings on Plastic Substrates*, 2001; Vol. 392.

(18) Cesarini, G.; Leahu, G.; Grilli, M. L.; Sytchkova, A.; Sibilia, C.; Li Voti, R. *Physica Status Solidi (C) Current Topics in Solid State Physics* **2016**, *13*, 998.

(19) Liu, S. Y.; Lian, L.; Pan, J.; Lu, J. G.; Shieh, H. P. D. *IEEE Transactions on Electron Devices* **2018**, *65*, 1939.

(20) Xu, M.; Qi, J.; Li, F.; Zhang, Y. *Journal of Materials Science* **2018**, *53*, 9589.

(21) Zhang, D.; Murakami, R. I. *International Journal of Modern Physics B* **2018**.

(22) Neves, A. I. S.; Bointon, T. H.; Melo, L. V.; Russo, S.; de Schrijver, I.; Craciun, M. F.; Alves, H. *Scientific Reports* **2015**, *5*, 9866.

(23) Bagal, A.; Dandley, E. C.; Zhao, J.; Zhang, X. A.; Oldham, C. J.; Parsons, G. N.; Chang, C.-H. *Materials Horizons* **2015**, *2*, 486.

(24) Kobayashi, N.; Masumoto, H.; Takahashi, S.; Maekawa, S. *Scientific Reports* **2016**, *6*, 34227.

(25) MoolKyul, K.; Hyun, P. J.; Il, L. K.; Woo, C. J.; Joonho, B.; Kwon, J. B.; Seung, L. C. *physica status solidi (a)* **2015**, *212*, 2005.

(26) Alnassar Mohammed, Y.; Ivanov Yurii, P.; Kosel, J. *Advanced Electronic Materials* **2016**, *2*, 1600081.

(27) Pirota, K.; Hernández-Vélez, M.; Navas, D.; Zhukov, A.; Vázquez, M. *Advanced Functional Materials* **2004**, *14*, 266.

(28) Vázquez, M.; Basheed, G. A.; Infante, G.; Del Real, R. P. *Physical Review Letters* **2012**, *108*.

(29) Calle, E.; Jiménez, A.; Vázquez, M.; del Real, R. P. *Journal of Alloys and Compounds* **2018**, *767*, 106.

(30) Vázquez, M. In *Handbook of Magnetism and Advanced Magnetic Materials* 2007.

(31) Qin, F.; Peng, H.-X. *Progress in Materials Science* **2013**, *58*, 183.

(32) Martins, P.; Lasheras, A.; Gutierrez, J.; Barandiaran, J.; Orue, I.; Lanceros-Mendez, S. *Journal of Physics D: Applied Physics* **2011**, *44*, 495303.

(33) Martins, P.; Gonçalves, R.; Lanceros-Mendez, S.; Lasheras, A.; Gutiérrez, J.; Barandiarán, J. M. *Applied Surface Science* **2014**, *313*, 215.

(34) Ribeiro, C.; Costa, C. M.; Correia, D. M.; Nunes-Pereira, J.; Oliveira, J.; Martins, P.; Gonçalves, R.; Cardoso, V. F.; Lanceros-Méndez, S. *Nature Protocols* **2018**, *13*, 681.